# Three-dimensional thermal simulations of thin solid carbon foils for charge stripping of high current uranium ion beams at a proposed new heavy-ion linac at GSI

N. A. Tahir,[1] V. Kim,[2] B. Schlitt,[1] W. Barth,[1] L. Groening,[1] I. V. Lomonosov,[2] A. R. Piriz,[3] Th. Stöhlker,[4] and H. Vormann[1]

[1]*GSI Helmholtzzentrum für Schwerionenforschung, Planckstraße 1, 64291 Darmstadt, Germany*
[2]*Institute of Problems of Chemical Physics, Russian Academy of Sciences, Institutskii Prospekt 18, 142432 Chernogolovka, Russia*
[3]*E.T.S.I.Industriales, Universidad de Castilla-La Mancha, 13071 Ciudad Real, Spain*
[4]*IOQ, Friedrich-Schiller-Universität, 07743 Jena, Germany; HelmholtzInstitut Jena, 07743 Jena, Germany; and GSI Helmholtzzentrum für Schwerionenforschung, Planckstraße 1, 64291 Darmstadt, Germany*

(Received 4 September 2013; published 28 April 2014)

This paper presents an extensive numerical study of heating of thin solid carbon foils by 1.4 MeV/u uranium ion beams to explore the possibility of using such a target as a charge stripper at the proposed new Gesellschaft für Schwerionenforschung high energy heavy–ion linac. These simulations have been carried out using a sophisticated 3D computer code that accounts for physical phenomena that are important in this problem. A variety of beam and target parameters have been considered. The results suggest that within the considered parameter range, the target will be severely damaged by the beam. Thus, a carbon foil stripper does not seem to be a reliable option for the future Gesellschaft für Schwerionenforschung high energy heavy–ion linac, in particular, at FAIR design beam intensities.

DOI: 10.1103/PhysRevSTAB.17.041003 PACS numbers: 29.27.-a

## I. INTRODUCTION

GSI Helmholtzzentrum für Schwerionenforschung (Gesellschaft für Schwerionenforschung), Darmstadt is a well known accelerator laboratory worldwide with advanced accelerator facilities that accelerate intense ion beams of all stable species from protons up to uranium. Construction of the new huge international accelerator complex, Facility for Antiproton and Ion Research (FAIR) [1], will allow scientists to study various interesting areas of physics including production of radioactive beams [2–6], high energy density (HED) physics [7–14], and the investigation of extreme states of matter [15]. Moreover, intense heavy ion beams are also considered to be a very efficient driver for inertial confinement fusion (ICF) [16–22]. This shows that intense ion beams are a very versatile, modern tool to research numerous important branches of basic and applied physics. In all the above cases, the experiments rely on the highest possible beam luminosities which constitutes a real challenge for the design and operation of the facility. This holds true for all beam handling and manipulation procedures, for example, charge stripper targets, electron cooling, acceleration in synchrotrons, where beam losses and dynamic vacuum effects need to be minimized, see for example [23,24]. Moreover, beam stability is a further important requirement.

At the GSI, the conventional Alverez type drift tube linac (DTL) providing acceleration from 1.4 MeV/u to 11.4 MeV/u has been in operation at the UNILAC (Universal Linear Accelerator) for about four decades [25]. As FAIR will need reliable injector linacs for the upcoming decades, it is proposed to replace the existing Alvarez type DTL by a newly designed linac. First design studies were performed comprising six interdigital H-mode (IH) DTL cavities [26,27] as depicted in Fig. 1. Table I lists the basic design parameters of this proposed new high energy (HE) heavy–ion linac. The baseline layout foresees to remain with the current gaseous ion charge stripper [28] at the entrance to the new DTL. Although the HE-Linac is designed to provide all ions except protons, the operation with uranium ion beams is the most demanding with respect to the machine design. For this reason we focus on this ion species in the present work. The present gas stripper comprises a supersonic gas jet of nitrogen crossing the incoming beam of 1.4 MeV/u $U^{4+}$. After the stripper, the mean charge state of $U^{28+}$ is separated through a dispersive section including two stages of horizontal collimation. After redeflection onto the initial beam axis, the beam is injected into the DTL. The operating rf frequency of the present DTL is 108 MHz. The proposed new HE-linac will use this frequency up to 11.4 MeV/u. For possible future beam energy upgrades, enhancement of

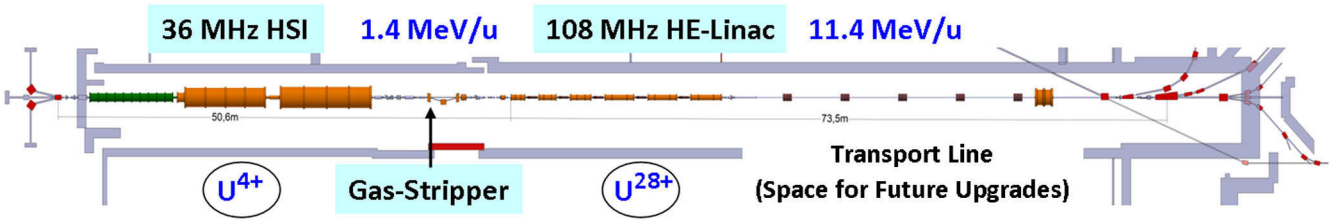


FIG. 1. Scheme of the proposed new GSI high energy heavy–ion linac.

the acceleration efficiency can be achieved by tripling the rf frequency to 325 MHz, thus allowing for operation of a newly developed crossed-bar H-mode (CH) DTL cavities. Similar CH–DTL cavities will also be used at 325 MHz in the upcoming FAIR proton linac [29].

The acceleration efficiency can be further increased by operation of the DTL and of the subsequent synchrotron with a higher charge state with respect to $U^{28+}$, as for example, $U^{39+}$. To compensate for increased space charge effects at synchrotron injection caused by the higher charge state, $U^{39+}$ should be accelerated in the injector linac to final energies of about 22–23 MeV/u. The $U^{39+}$ scenario may also be an option for a major upgrade of the HE-linac. This upgrade may foresee to skip injection into the 18 Tm synchrotron SIS18 and rather inject directly into the 100 Tm synchrotron SIS100 at about 100–150 MeV/u. Applying an increase of energy and of charge state, the beam quality deterioration effects due to the beam charge self-forces and beam stripping from residual gas interaction (dynamic vacuum effects) can be significantly mitigated.

Such a HE linac upgrade to higher charge states must be based on a reliable, durable, and stable charge stripping technique comparable to the present gaseous stripper. The effect of the charge stripper on the beam properties should not change with time since any variation of the latter will require continuous readjustment of the operation parameters of the subsequent accelerator sections, or it will cause unstable beam conditions for any facility at FAIR. These are very crucial demands, in particular, since for FAIR design beam intensities the stripper target at 1.4 MeV/u has to bear a very high ion beam power of 1.5 MW for 18 emA $U^{4+}$ beams during short beam pulses ($\leq 100$ $\mu$s) at low duty cycle (2.7 Hz beam repetition rate).

Thus, different approaches are being investigated at the UNILAC to generate higher charge states and to increase the stripping efficiency [27,30–33]. One option could be to replace the gas stripper by a thin solid carbon stripper foil. Various experiments with different types of stripping foils and ion beams were performed at the UNILAC during the past years [30–32]. For a better understanding of the experimental results, extensive numerical simulations of the stripper foil heating by uranium ion beams have been performed and are presented in this paper.

In Sec. II we report some experimental results that have been achieved with $U^{4+}$ beams using thin carbon foils as a stripping medium at the existing UNILAC. In Sec. III we present beam and stripper parameters that have been used in the extensive theoretical studies. The simulations are reported in Sec. IV, while the conclusions drawn from this work are noted in Sec. V.

TABLE I. Main parameters of the proposed new high energy (HE) heavy–ion drift tube linac at GSI.

| | |
|---|---|
| Ion | $U^{28+}/U^{39+}$ (baseline/upgrade) |
| Input energy | 1.4 MeV/u |
| Output energy | 11.4/≈22–23 MeV/u |
| Ion current | 15 emA/21 emA |
| Beam pulse length | $\leq 100$ $\mu$s |
| Repetition rate | 2.7 Hz |

## II. EXPERIMENTAL RESULTS OF RECENT FOIL–STRIPPER OPERATION AT THE UNILAC

As an example, Fig. 2 shows photographs of thin self-supporting carbon foils being irradiated by 1.4 MeV/u $U^{4+}$ beams at electrical beam currents of about 5–6 emA for typically four hours (100 $\mu$s, 2 Hz beam pulses) while the focal spot rms radius ≈5 mm. Mainly ≈20 $\mu g/cm^2$ thick amorphous carbon foils produced at the GSI target laboratory [34,35] as well as those provided by Isao Sugai from KEK, were used [30–32]. Some thicker foils of 30–50 $\mu g/cm^2$ were also considered.

Most of the foils were damaged after irradiation [30–32]. The pattern of damages reaches from just warped surface after seeing some 30000 shots to full destruction after few shots. Most of the foils featured holes at the location of maximum beam intensity and the measured stripping efficiency decreased significantly with the duration of irradiation. A logical explanation for these results is that even if the foil is not heated to the sublimation temperature, the foil is damaged after being irradiated a number of times due to material fatigue and stress induced effects (thermal and mechanical stresses and stress waves induced in the foils by the short intense beam pulses [36]). Different post irradiation investigations by the GSI material physics department also indicate a partial conversion of amorphous carbon to polycrystalline graphite at high temperatures in the target center leading to in-plane tensile stresses due to the high density of the crystalline phase [36].

A mean charge state around $U^{39+}$ was observed behind the stripping foils, for measured charge distributions see

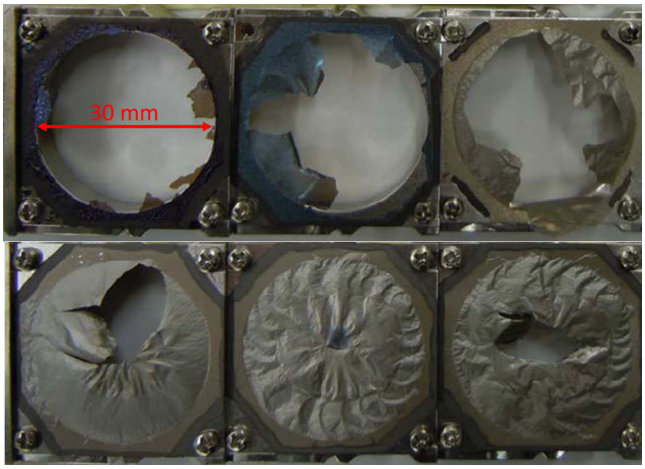


FIG. 2. Damage shown to solid carbon stripper foils irradiated by 5–6 emA of $U^{4+}$ with a rms focal spot radius ≈5 mm, the foils were made mainly at the GSI target laboratory.

Refs. [30,31]. Beam energy measurements behind the charge separator showed no distinct change of the energy loss in the stripping foil during irradiation. Typical values range between 17 keV/u and 22 keV/u for a foil thickness around $\approx 20\ \mu g/cm^2$. Beam emittance measurements behind the charge separator showed also no considerable variation during irradiation.

A significant dependence of the foil lifetime on the ion beam pulse length was observed. Foils irradiated with beam pulses of 50–100 $\mu$s length showed significantly longer lifetimes than foils irradiated with 50% longer beam pulses. Generally, the lifetimes of the $20\ \mu g/cm^2$ foils were considerably longer compared to the thicker foils.

Several foil production and preparation methods were tested using carbon material from different suppliers. However, for the time being, no reproductive correlation among these different methods could be established. The most commonly used method for production of thin carbon foils at GSI employs resistance evaporation technique under high vacuum [34,35]. A carbon rod which is fixed between two electrodes is heated by resistance heating, the carbon sublimates and is deposited on substrate plates which are arranged concentrically around the rod. Since a water-soluble interlayer is used between the glass substrate and the carbon film, the carbon layer can be taken off the substrate in distilled water by dissolving the interlayer. The remaining carbon sheets can be picked up with suitable target frames. Thus, tension-free self-supporting carbon thin films with thicknesses from $5\ \mu g/cm^2$ up to $50\ \mu g/cm^2$ can be obtained. Further details about foil production techniques can be found in [34,35].

## III. BEAM AND STRIPPER PARAMETERS USED IN THEORETICAL STUDIES

In order to have a better understanding of these experimental results and to assess the feasibility of using a solid stripper in the new GSI high energy drift tube linac, we have done an extensive parameter study of beam-matter heating. The stripper is assumed to be a thin circular foil of solid graphite with density $2.28\ \mu g/cm^3$ and radius, $R_f = 1.5$ cm while the uranium beam is incident perpendicular to its surface. Three different foil thicknesses including 20, 30, and 40 $\mu g/cm^2$, respectively, have been considered.

The initial mean charge state is $U^{4+}$ while the ion is stripped to a mean charge state of $U^{39+}$ after passing through either 20 or 30 $\mu g/cm^2$ thick stripper foils. A slightly higher charged state of $U^{40+}$ is achieved with a 40 $\mu g/cm^2$ thick foil. For simplicity, we assume in the calculations a uniform ion charge state along the foil thickness (39+ in case of 20 and 30 $\mu g/cm^2$ and 40+ in case of 40 $\mu g/cm^2$ thickness). In practice, however, there will be a certain charge distribution along the ion trajectory as well as around the mean charge state. According to Figs. 8 and 9, exponential charge distribution along the ion path leads to a higher temperature compared to a linear charge distribution when thermal conduction is considered. Since the uniform charge distribution results in temperatures comparable to more realistic exponential charge distribution (see Sec. IV A), the uniform distribution is used to simplify the simulations.

Ion energy is taken to be 1.4 MeV/u while two different values of the beam current, namely, 6 emA and 18 emA have been used. It is to be noted that 18 emA is the FAIR design value of the beam current whereas 6 emA corresponds to the experiments performed so far.

A pulse length of 100 $\mu$s is considered that leads to pulse intensities, $N = 9.375 \times 10^{11}$ and $2.8125 \times 10^{12}$ for the beam current values of 6 emA and 18 emA, respectively.

The transverse particle distribution in the focal spot is assumed to be Gaussian with $\sigma = 3.67$ mm, whereas the repetition rate of the ion beam pulses is 2 Hz.

## IV. NUMERICAL SIMULATION RESULTS

In this section we present numerical simulation results of the thermal response of a solid carbon stripper foil irradiated by a uranium beam using various sets of parameters noted in Sec. III. It is to be noted that in this work we are only interested in studying the target heating, excluding any hydrodynamics. These simulations have been carried out using an upgraded version of a 3D simulation code, PIC3D [37], that is based on a finite-size particle-in-cell algorithm that includes ion energy deposition as well as heat conduction. An advanced equation of state (EOS) model [38] is used to treat different phases of carbon in the target. The upgraded version additionally includes thermal radiation losses from the target surface which is very important in the present type of problem [39]. We note that similar studies have previously been done for the low energy, light ion beams to be generated at the SPIRAL2, and the results are reported elsewhere [39,40].

It is to be noted that generating a high resolution three-dimensional mesh for such very thin targets is very complicated. To overcome this problem, the disc area (at the middle of the thickness) is discretized in a two-dimensional numerical mesh, whereas along the foil thickness, we assume a parabolic temperature profile to take into account surface cooling due to the radiation losses. The problem is solved iteratively using Newton–Raphson method thereby ensuring the convergence of the solution. Further details can be found in the appendix of Ref. [39].

### A. Beam current 6 emA and pulse length 100 $\mu$s

The above beam parameters lead to a pulse intensity, $N = 9.375 \times 10^{11}$. For the simplicity of calculations, we assume a parabolic temporal profile for the beam power, although in practice the profile is more complicated. This however, is not so important as the final temperature depends on the total energy absorbed by the target. For radiation loss calculations, an emissivity, $\epsilon = 0.9$ is used.

First, we consider a foil thickness of 20 $\mu$g/cm$^2$. The SRIM code [41] has been used to calculate the energy loss of ions in the target. It is to be noted that the SRIM model assumes a fully stripped ion which means an effective ion charge, $Z_{\mathrm{eff}} = 92$ for uranium. However, the effective charge on the stripped ion, in the present case, is $Z_{\mathrm{strip}} = 39$. It is well known that the ion energy loss in matter is proportional to $Z^2_{\mathrm{eff}}$ [42]. Therefore to take this effect into account, we multiply the SRIM energy loss data by the ratio $Z^2_{\mathrm{strip}}/Z^2_{\mathrm{eff}}$, which is 0.18.

In Fig. 3 we plot the temperature at three different points along the foil radius, namely, $r = 0$ (center), 5 mm, and 15 mm (outer boundary), respectively. It is seen that a maximum temperature of around 2200 K is achieved at the target center at the end of the pulse (100 $\mu$s), whereas the maximum temperature at $r = 5$ mm is about 1250 K. The temperature at the foil boundary, on the other hand, does not change. It is to be noted that although the sublimation temperature of carbon in air is much higher (3925 K), the target could be damaged due to the induced thermal and mechanical stresses [3–5,36]. It is also worth mentioning that the sublimation temperature of carbon in vacuum is even lower [43]. At the maximum temperature of 2200 K (Fig. 3) the carbon sublimation pressure is about $10^{-6}$ mbar [43], which is in the order of or even larger than the vacuum pressure in the beam pipe around the foil stripper. Hence, sublimation can be an issue in the foil center at the end of the ion beam pulse in the cases investigated in this paper.

It is also seen from Fig. 3 that as the beam is switched off, the temperature starts to decrease at both points. It is interesting to note that the rate of decrease of the temperature is higher at $r = 0$ compared to $r = 5$ mm. This is due to the fact that the radiation loss rate is proportional to the fourth power of the temperature. Since the temperature at the foil center is higher than at $r = 5$ mm, the former cools down faster than the latter.

In Fig. 4 we present target temperature vs time at the foil center ($r = 0$) using a beam pulse repetition rate = 2 Hz for the same beam and target parameters as in Fig. 3. It is seen that the target temperature is reduced to the room temperature within 5 ms and the target is completely cooled before it is irradiated again that shows that there will be no accumulation of heat. Therefore if the stripper foil survives one impact, it will survive operation with a frequency of 2 Hz.

It is worth mentioning that the emissivity is an important parameter in the radiation loss calculations. In the present work we assume an emissivity of 0.9 for carbon, a value that is provided in the literature. However, in experiments performed at the GSI [44], the experimentally measured value of the emissivity for very thin carbon foils (thickness 20 $\mu$g/cm$^2$) is found to be 0.2. In order to check the

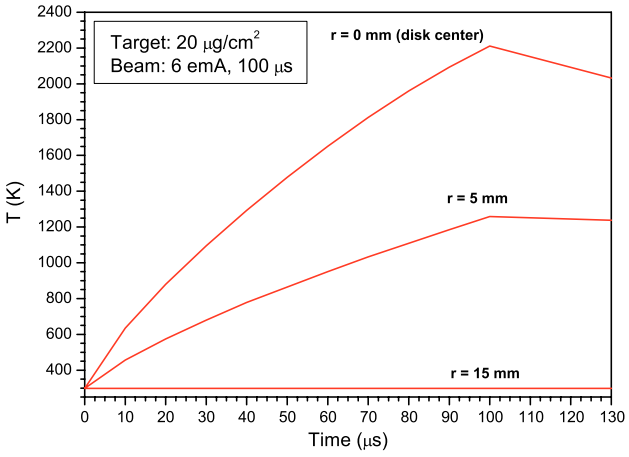


FIG. 3. Temperature vs time (during pulse length) at three different points along foil radius, foil thickness = 20 $\mu$g/cm$^2$, beam current 6 emA, and pulse length = 100 $\mu$s.

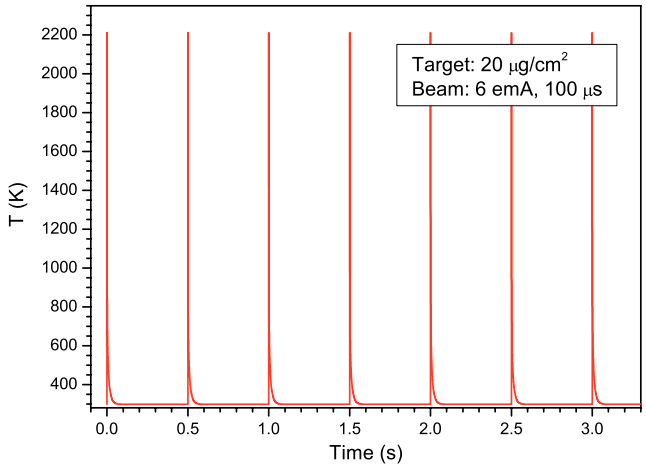


FIG. 4. Temperature vs time at foil center ($r = 0$), beam pulse repetition rate = 2 Hz, foil thickness = 20 $\mu$g/cm$^2$, beam current 6 emA, and pulse length = 100 $\mu$s.

influence of emissivity on the foil cooling we repeated the above calculations using $\epsilon = 0.2$ and the results are presented in Fig. 5 where we plot the temperature at the foil center vs time using the two different values of $\epsilon$. It is interesting to see that the final temperature at $r = 0$ in the two cases differs only by 8%, whereas the emissivity differs by a factor of 4.5. This is because the radiation loss rate is linearly proportional to the emissivity, but is proportional to the fourth power of the temperature [39]. Therefore the effect of reduction in the emissivity on the radiation loss is compensated by an increase of temperature much more rapidly. However, after $t = 100$ $\mu$s, the two curves show a different behavior.

The cooling rate is faster for higher emissivity. This can be further illustrated in Fig. 6, where we present the temperature at the foil center for a longer time. It is seen that the cooling time is increased to around 150 ms for $\epsilon = 0.2$ instead of 50 ms in the other case. Nevertheless, the target is still cooled to the room temperature before it is irradiated again. It is thus concluded that our results are insensitive to large variation in the emissivity. We therefore use $\epsilon = 0.9$ in this study.

Figure 7 presents the same parameters as in Fig. 3, but using a foil thickness of 30 $\mu$g/cm$^2$. It is seen that the maximum temperature is somewhat higher than in Fig. 3 because, due to the larger thickness of the target in the present case, the diffusion of heat from the target center to the surface takes a longer time that reduces the cooling rate.

In order to study the effect of nonuniform ion charge distribution along the ion trajectory, we have carried out calculations using a linear as well as an exponential charge distribution. In this case we perform one-dimensional simulations along the thickness at one point on the surface (the foil center) using a high resolution numerical mesh. In Fig. 8 we present results considering a linear charge distribution along the foil thickness. The material internal energy and the temperature resulting from the energy deposition are presented along the foil axis at $t =$ 100 $\mu$s (end of the pulse). The solid lines correspond to the case when no thermal conduction is included, whereas the dashed lines represent the case when thermal conduction is allowed as well. It is interesting to note that the temperature becomes very uniform along the foil thickness due to the thermal conduction and full thermalization is achieved on a very short time scale (within the pulse duration). The maximum temperature in this case is around 1250 K which is significantly lower than in the case when a uniform charge state is considered along the foil thickness. It is to be noted that the outer shell electrons are more loosely bound to the atom compared to the inner shell electrons. This leads to a very rapid ionization of the projectile ion during the early part of its trajectory through the stripper foil until an equilibrium charge state is rapidly achieved. The ion charge distribution therefore resembles more closely an exponential distribution rather than a linear distribution. Measurements of the mean charge state as a

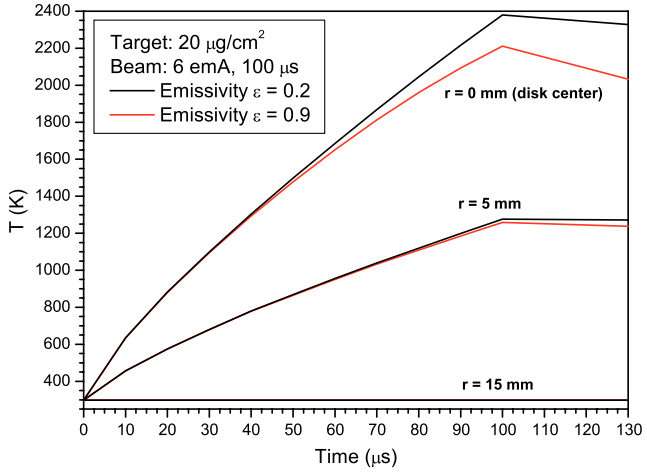


FIG. 5. Temperature vs time using $\epsilon = 0.2$ and 0.9 for the case in Fig. 3.

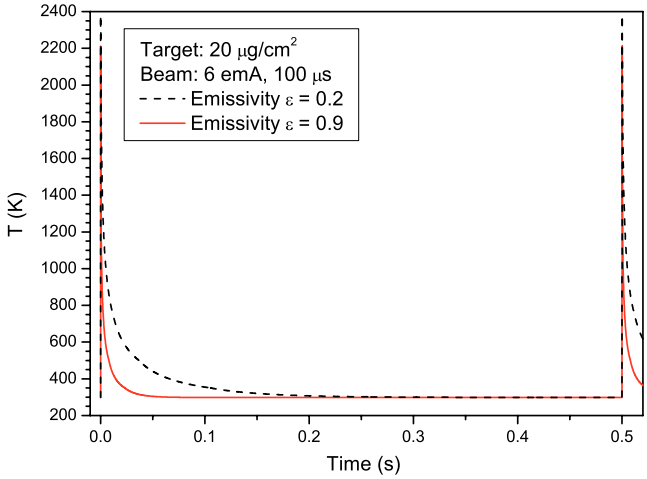


FIG. 6. Same as in Fig. 5, but for a longer time.

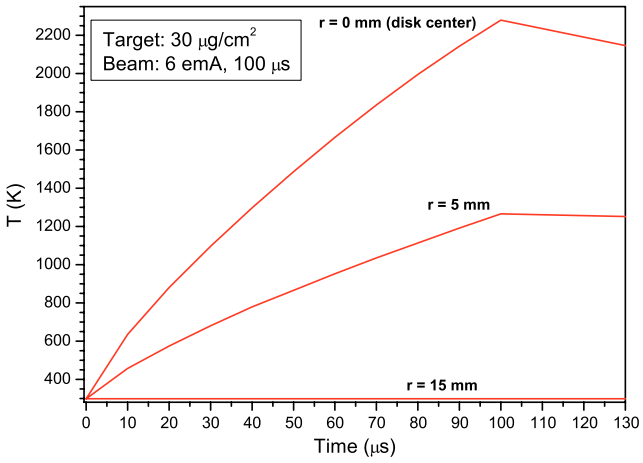


FIG. 7. Same as in Fig. 3, but for foil thickness = 30 $\mu$g/cm$^2$.

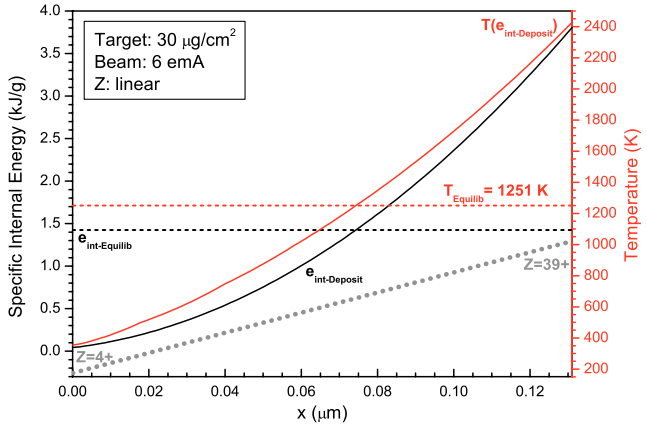


FIG. 8. Linear ion charge distribution along ion trajectory: temperature and internal energy along the beam axis at $t = 100\ \mu s$ (end of the pulse), solid lines represent exclusion of heat conduction and dashed lines represent inclusion of heat conduction, foil thickness $= 30\ \mu g/cm^2$, ion current $= 6$ emA, particle energy $= 1.4$ MeV/u.

function of the carbon foil thickness for copper and nickel projectile ions [45] also show a charge evolution which agrees well with an exponential approximation.

In Fig. 9 we present the same variables as in Fig. 8, but using an exponential charge distribution along the target thickness. It is seen that including the heat conduction, a uniform temperature of 2165 K is obtained along the target axis, which is close to that in Fig. 7. It is therefore concluded that the stripper foil will be strongly heated and may be permanently damaged by the induced thermal stresses.

In Fig. 10 we present the same parameters as in Fig. 3, but using a foil thickness of 40 $\mu g/cm^2$. In this case we only consider a uniform charge distribution of 40+ along the target thickness. It is seen that the maximum temperature at the target axis at the end of the pulse is around 2400 K, which is slightly higher than in Fig. 3.

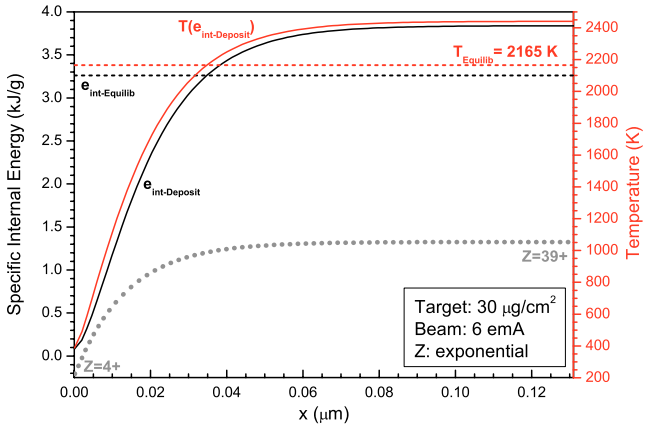


FIG. 9. Same as in Fig. 8, but using an exponential ion charge distribution.

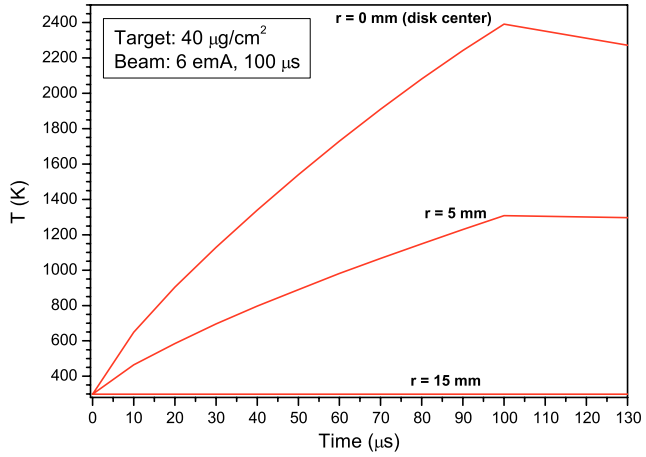


FIG. 10. Same as in Fig. 3, but for foil thickness $= 40\ \mu g/cm^2$ and a uniform charge distribution of 40+.

### B. Beam current 18 emA and pulse length 100 $\mu$s

In this section we present the calculations using the higher value of the beam current for the above three different foil thicknesses. Again we use a $\epsilon = 0.9$, beam pulse repetition rate $= 2$ Hz, and a uniform ion charge distribution along the foil thickness.

It is seen in Fig. 11 that in the case of a 20 $\mu g/cm^2$ thick stripper foil, a maximum temperature of about 3300 K is achieved along the axis. It is also seen that the temperature rises linearly up to 60 $\mu$s and then the rate of increase decreases gradually due to the excessive radiation losses at higher temperature. A similar behavior is seen in Figs. 12 and 13 where the corresponding temperature is about 3700 K and 4000 K, respectively. These results demonstrate that a solid carbon stripper foil will not survive even a single irradiation with the beam current of 18 emA. It is to be noted that in the case of foil thickness $= 40$ g/cm$^2$ we consider a uniform charge distribution of 40+ along the target thickness.

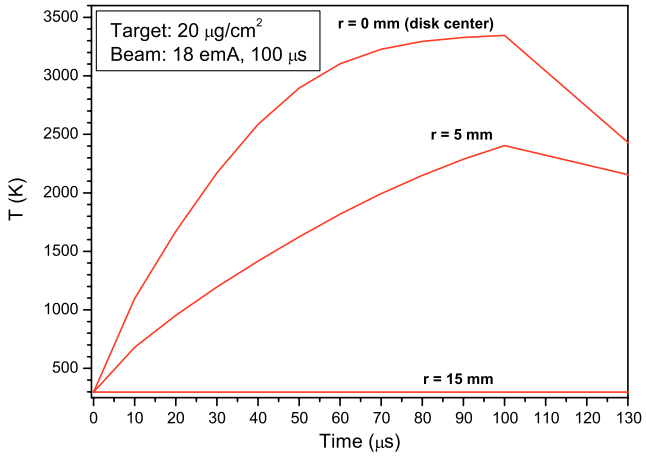


FIG. 11. Same as in Fig. 3, but using beam current of 18 emA.

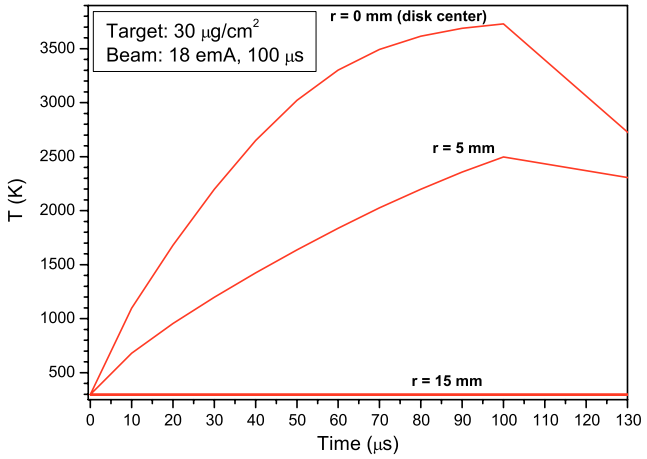


FIG. 12. Same as in Fig. 11, but for foil thickness = 30 $\mu g/cm^2$.

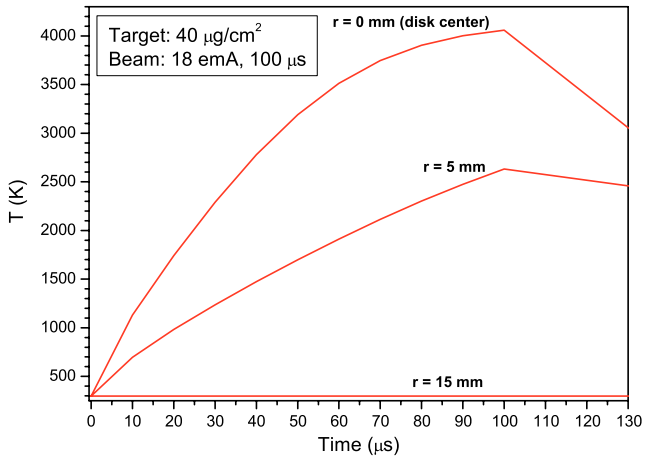


FIG. 13. Same as in Fig. 11, but for foil thickness = 40 $\mu g/cm^2$ using a uniform charge distribution of 40+.

It is to be noted that the energy deposition in the stripping foils is reduced by emission of ion-induced electrons from the foil surfaces. Measured electron yields and electron energies following the impact of 3.5 MeV/u $U^{38+}$ and 8 MeV/u $U^{68+}$ ions on 44 $\mu g/cm^2$ carbon foil targets were reported in [46]. The total electron yields amount to about 1900 and 2500 electrons per incident ion, respectively, with mean electron energies ranging from 240 eV in the backward direction to 880 eV in the forward direction. Scaling laws for electron yields and for electron energies depending on target thickness as well as on the projectile energies are given in [45,47], considering also the transport length for fast and for slow secondary electrons.

In our case of 1.4 MeV/u $U^4+$ ion beams and 20–40 $\mu g/cm^2$ carbon foils, we conclude that both charge-state equilibrium and complete development of the secondary electron cascades are reached and the approximations for the thick target can be used. Extrapolating the data from [46] to 1.4 MeV/u uranium ion beams, using these scaling laws and measured dE/dx of uranium ions in carbon foils reported in [48], we estimate a total electron yield in the order of 1600 electrons per projectile ion. This leads to a total energy of around 250 keV per incident ion removed from the target due to electron emission. Taking into account a reasonable uncertainty, this corresponds to about 5%–10% of the energy loss of the projectile ions in the carbon foil. Since the foil temperature scales as square root of the specific energy deposition, the change in the temperature will be smaller than the change in the energy deposition. Thus reduction in temperature caused by the electron emission from the foil surface will be of smaller order than the increase caused by lower emissivity. Hence it is concluded that the electron emission effects are within the level of accuracy of the numerical simulations reported in this paper and are thus neglected in the simulations results. The overall conclusions that the foils will be heated to above 2000 K and will be finally destroyed due to thermal stresses are not affected by electron emission.

## V. CONCLUSIONS

We report numerical simulations of the thermal response of thin solid carbon foils irradiated by a uranium ion beam. These simulations have been carried out using a sophisticated 3D computer code that is equipped with ion energy deposition, heat conduction, and thermal radiation losses from the target surface. Different phases of the target material are handled by using an advanced multiphase, multicomponent EOS package [38]. A wide range of beam and target parameters has been considered. The stripper is assumed to be a thin foil of solid carbon with radius = 15 mm while three different thicknesses, namely, 20, 30, and 40 $\mu g/cm^2$, respectively, have been considered. Two different uranium beam current values including 6 and 18 emA, have been considered whereas the pulse length is taken to be 100 $\mu s$. Pulse repetition rate is assumed to be 2 Hz in all the cases. The transverse ion intensity distribution in the focal spot is Gaussian with $\sigma = 3.67$ mm.

The results have shown that in the case of the higher beam current of 18 emA, at the foil center where the maximum of the Gaussian is located, the temperature at $t = 100\,\mu s$ (end of the ion pulse) exceeds the sublimation temperature of carbon in vacuum even in a single irradiation. This means that the foil will be severely damaged due to the creation of a hole in that region. In case of the lower beam current of 6 emA, the maximum temperature is close to the sublimation temperature of carbon in vacuum. Nevertheless the induced thermal stresses and the material fatigue will finally result in damage after a certain number of irradiations as observed in the experiments (see Fig. 2). It is therefore concluded that the use of a solid stripper foil is not feasible at the new high energy drift tube linac at GSI.

## ACKNOWLEDGMENTS

The authors wish to thank G. I. Kerley (the Sandia National Laboratories) for providing the multiphase, multicomponent EOS data for carbon. We also wish to thank M. Tomut (GSI, Darmstadt) for providing information concerning the measured emissivity of thin carbon foils. Many thanks to H. Weick (GSI, Darmstadt) for his support regarding the discussion of the charge state evolution of the projectile ions along their trajectory in the foils as well as the estimate of the energy taken away by secondary electrons.

[1] FAIR baseline Technical Report No. ISBN 3–9811298–0–6, GSI, Darmstadt, Germany, 2006.

[2] H. Geissel, H. Weick, M. Winkler, G. Münzenberg, V. Chichkine, M. Yavor, T. Aumann, K. A. Behr, M. Bohmer, A. Brunle, K. Burhard, J. Benlliure, D. Gill-Cortina, L. Chulkov, A. Dael, J. E. Ducret, H. Emling, B. Franczak, J. Friese *et al.*, Nucl. Instrum. Methods Phys. Res., Sect. B **204**, 71 (2003).

[3] N. A. Tahir, V. Kim, A. V. Matveichev, A. V. Ostrik, A. V. Sultanov, I. V. Lomonosov, A. R. Piriz, J. J. Lopez Cela, and D. H. H. Hoffmann, Laser Part. Beams **26**, 273 (2008).

[4] N. A. Tahir, H. Weick, A. Shutov, V. Kim, A. V. Matveichev, A. V. Ostrik, A. V. Sultanov, I. V. Lomonosov, A. R. Piriz, J. J. Lopez Cela, and D. H. H. Hoffmann, Laser Part. Beams **26**, 411 (2008).

[5] N. A. Tahir, A. Matveichev, V. Kim, A. V. Ostrik, A. Shutov, V. Sultanov, I. V. Lomonosov, A. R. Piriz, and D. H. H. Hoffmann, Laser Part. Beams **27**, 9 (2009).

[6] T. Aumann, K. Langanke, K. Peters, and Th. Stöhlker, Eur. Phys. J. Web Conf. **3**, 01006 (2010).

[7] N. A. Tahir, C. Deutsch, V. E. Fortov, V. Gryaznov, D. H. H. Hoffmann, M. Kulish, I. V. Lomonosov, V. Mintsev, P. Ni, D. Nikolaev, A. R. Piriz, N. Shilkin, P. Spiller, A. Shutov, M. Temporal, V. Ternovoi, S. Udrea, and D. Varentsov, Phys. Rev. Lett. **95**, 035001 (2005).

[8] N. A. Tahir, D. H. H. Hoffmann, A. Kozyreva, A. Tauschwitz, A. Shutov, J. A. Maruhn, P. Spiller, U. Neuner, J. Jacoby, M. Roth, R. Bock, H. Juranek, and R. Redmer, Phys. Rev. E **63**, 016402 (2000).

[9] N. A. Tahir, A. Kozyreva, P. Spiller, D. H. H. Hoffmann, and A. Shutov, Phys. Rev. E **63**, 036407 (2001).

[10] N. A. Tahir, A. Shutov, D. Varentsov, P. Spiller, S. Udrea, D. H. H. Hoffmann, I. Lomonosov, J. Wieser, M. Kirk, R. Piriz, V. E. Fortov, and R. Bock, Phys. Rev. ST Accel. Beams **6**, 020101 (2003).

[11] N. A. Tahir, P. Spiller, S. Udrea, O. D. Cortazar, C. Deutsch, V. E. Fortov, V. Gryaznov, D. H. H. Hoffmann, I. V. Lomonosov, P. Ni, A. R. Piriz, A. Shutov, M. Temporal, and D. Varentsov, Nucl. Instrum. Methods Phys. Res., Sect. B **245**, 85 (2006).

[12] A. R. Piriz, J. J. Lopez Cela, M. C. Serna Moreno, N. A. Tahir, and D. H. H. Hoffmann, Laser Part. Beams **24**, 275 (2006).

[13] A. R. Piriz, O. D. Cortazar, J. J. Lopez Cela, and N. A. Tahir, Am. J. Phys. **74**, 1095 (2006).

[14] A. R. Piriz, J. J. Lopez Cela, and N. A. Tahir, Phys. Rev. E **80**, 046305 (2009).

[15] Th. Stöhlker, H. F. Beyer, H. Brauning, A. Brauning-Demian, C. Brandau, S. Hagmann, C. Kozhuharov, H. J. Kluge, Th. Khl, D. Liesen, R. Mann, W. Nörtershauser, W. Quint, U. Schramm, and R. Schuch, Nucl. Instrum. Methods Phys. Res., Sect. B **261**, 234 (2007).

[16] R. O. Bangerter, J. W. K. Mark, and A. R. Thiessen, Phys. Lett. A **88**, 225 (1982).

[17] A. R. Piriz, Phys. Fluids **31**, 658 (1988).

[18] C. Deutsch, Ann. Phys. (Paris), **11**, 1 (1986).

[19] B. G. Logan, L. J. Perkins, and J. J. Barnard, Phys. Plasmas **15**, 072701 (2008).

[20] N. A. Tahir and K. A. Long, Phys. Lett. A **90**, 242 (1982).

[21] N. A. Tahir and K. A. Long, Laser Part. Beams **2**, 371 (1984).

[22] N. A. Tahir and K. A. Long, Z. Phys. A **325**, 99 (1986).

[23] O. Boine-Frankenheim, *Proceedings of the International Particle Accelerator Conference, Kyoto, Japan* (ICR, Kyoto, 2010), p. 2430.

[24] R. E. Olson, R. L. Watson, V. Horvat, K. E. Zaharakis, R. D. DuBois, and Th. Stöhlker, Nucl. Instrum. Methods Phys. Res., Sect. B **544**, 333 (2005).

[25] D. Böhne, in *Proceedings of the 1976 Proton Linear Accelerator Conference, Chalk River, Ontario, Canada* (Atomic Energy of Canada, 1976), p. 2.

[26] B. Schlitt, G. Clemente, W. Barth, and W. Vinzenz, GSI Scientific Report 2012, Report No. GSI-2013-1, 2013.

[27] B. Schlitt, G. Clemente, W. Barth, and W. Vinzenz, in *Proceedings of the 12th Heavy Ion Accelerator Technology Conference (HIAT2012), Chicago, Illinois, USA*, p. 191.

[28] W. Barth and P. Forck, in *Proceedings of the 20th International Linac Conference, LINAC-2000, Monterey, CA, 2000* (SLAC, Menlo Park, CA, 2000), p. 235.

[29] G. Clemente, U. Ratzinger, H. Podlech, L. Groening, R. Brodhage, and W. Barth, Phys. Rev. ST Accel. Beams **14**, 110101 (2011).

[30] W. Barth, G. Clemente, P. Gerhard, L. Groening, B. Lommel, M. S. Kaiser, M. Maier, S. Mickat, W. Vinzenz, and H. Vormann, in *Proceedings of the 25th International Linear Accelerator Conference, LINAC-2010, Tsukuba, Japan* (KEK, Tsukuba, Japan, 2010), p. 154.

[31] W. Barth, M. S. Kaiser, B. Lommel, M. Maier, S. Mickat, B. Schlitt, J. Steiner, M. Tomut, and H. Vormann, J. Radioanal. Nucl. Chem. **299**, 1047 (2014).

[32] H. Vormann, W. Barth, G. Clemente, L. Dahl, P. Gerhard, V. Gettmann, L. Groening, M. S. Kaiser, M. Maier, S. Mickat, A. Orzhekhovskaya, B. Schlitt, and S. Yaramyshev, "Unilac Machine Experiments in 2012," GSI, 2012 (unpublished).

[33] B. Schlitt, H. Vormann, W. Barth, G. Clemente, L. Groening, M. S. Kaiser, B. Lommel, M. Maier, S. Mickat, and J. Steiner, in *Proceedings of the 4th International Particle Accelerator Conference, IPAC-2013, Shanghai, China, 2013 (JACoW, Shanghai, China, 2013), p. 3779.*

[34] B. Lommel, W. Hartmann, B. Kindler, J. Klemm, and J. Steiner, Nucl. Instrum. Methods Phys. Res., Sect. A **480**, 199 (2002).

[35] W. Thalheimer, W. Hartmann, J. Klemm, and B. Lommel, Cryst. Res. Technol. **34**, 175 (1999).
[36] M. Tomut, O. Ersen, S. Moldovan, W. Barth, P. Gehard, M. S. Kaiser, B. Lommel, M. Maier, J. Steiner, H. Vormann, and C. Trautmann, "Failure Mode of Carbon Stripper Foils Exposed to Intense Heavy-Ion Beams," GSI, 2011 (unpublished).
[37] V. E Fortov, V. Kim, I. V. Lomonosov, A. Matveichev, and A. Ostrik, Int. J. Impact Eng. **33**, 244 (2006).
[38] G. Kerley, "Multi–Component, Multi–Phase Equation of State for Carbon," Sandia Nat. Lab, 2001 (unpublished).
[39] N. A. Tahir, V. Kim, E. Lamour, I. V. Lomonosov, A. R. Piriz, J. P. Rozet, Th. Stöhlker, V. Sultanov, and D. Vernhet, Nucl. Instrum. Methods Phys. Res., Sect. B **276**, 66 (2012).
[40] N. A. Tahir, V. Kim, E. Lamour, I. V. Lomonosov, A. R. Piriz, J. P. Rozet, Th. Stöhlker, V. Sultanov, and D. Vernhet, Nucl. Instrum. Methods Phys. Res., Sect. B **290**, 43 (2012).
[41] J. F. Ziegler, J. P. Biersack, and U. Littmark, *The Stopping and Ranges of Ions in Solids* (Pergamon, New York, 1996).
[42] C. Deutsch, Ann. Phys. (N.Y.) **11**, 1 (1986).
[43] P. Thieberger, Muon Collider Document MUC-0186, 2000.
[44] K. Kupka, M. Tomut, C. Hubert, R. Danjoux, B. Lommel, J. Steiner, and C. Trautmann, "Measurement of Carbon Stripper Foils Emissivity for Quantitative On-Line Infrared Thermography," GSI, 2012 (unpublished).
[45] M. Jung, H. Rothard, B. Gervais, J.-P. Grandin, A. Clouvas, and R. Wunsch, Phys. Rev. A **54**, 4153 (1996).
[46] D. Schneider, G. Schiwietz, and D. DeWitt, Phys. Rev. A **47**, 3945 (1993).
[47] H. Rothard, C Caraby, A. Cassimi, B. Gervais, J.-P. Grandin, P. Jardin, M. Jung, A. Billebaud, M. Chevallier, K.-O. Groeneveld, and R. Maier, Phys. Rev. A **51**, 3066 (1995).
[48] H. Geissel, H. Weick, C. Scheidenberger, R. Bimbot, and D. Gardes, Nucl. Instrum. Methods Phys. Res., Sect. B **195**, 3 (2002).